

Learning to synthesise the ageing brain without longitudinal data

Tian Xia*, Agisilaos Chartsias, Chengjia Wang, and Sotirios A. Tsafaris, for the Alzheimer’s Disease Neuroimaging Initiative

Abstract—Brain ageing is a continuous process that is affected by many factors including neurodegenerative diseases. Understanding this process is of great value for both neuroscience research and clinical applications. However, revealing underlying mechanisms is challenging due to the lack of longitudinal data. In this paper, we propose a deep learning-based method that learns to simulate subject-specific brain ageing trajectories *without* relying on longitudinal data. Our method synthesises aged images using a network conditioned on two clinical variables: age as a continuous variable, and health state, i.e. status of Alzheimer’s Disease (AD) for this work, as an ordinal variable. We adopt an adversarial loss to learn the joint distribution of brain appearance and clinical variables and define reconstruction losses that help preserve subject identity. To demonstrate our model, we compare with several approaches using two widely used datasets: Cam-CAN and ADNI. We use ground-truth longitudinal data from ADNI to evaluate the quality of synthesised images. A pre-trained age predictor, which estimates the apparent age of a brain image, is used to assess age accuracy. In addition, we show that we can train the model on Cam-CAN data and evaluate on the longitudinal data from ADNI, indicating the generalisation power of our approach. Both qualitative and quantitative results show that our method can progressively simulate the ageing process by synthesising realistic brain images.

Index Terms—brain ageing, generative adversarial network, neurodegenerative disease, magnetic resonance imaging (MRI)

I. INTRODUCTION

THE ability to predict the future status of an individual is able to offer preventive and prognostic clinical guidance [1]. Recently, deep generative models have been used to simulate and predict pathological processes within different clinical applications, for example, to synthesise the future degeneration of a human brain using existing scans [2]–[5]. However, to accomplish such accurate estimation for specific subjects, current methods require considerable amount of longitudinal data to sufficiently learn a complex auto-regression function. Here, we propose a new conditional adversarial training procedure that does *not* require longitudinal data to

train. Our model (illustrated in Fig. 1) synthesises images of aged brains for a specific age and health state.

Brain ageing, accompanied by a series of functional and physiological changes, has been intensively investigated [6], [7]. However, the underlying mechanism has not been completely revealed [8], [9]. Prior studies have shown that brain’s chronic changes are related to different factors, e.g., the biological age [10], degenerative diseases such as Alzheimer’s Disease (AD) [11], binge drinking [12], and even education [13]. Accurate simulation of this process has great value for both neuroscience research and clinical applications to identify age-related pathologies [9], [10]. In this work, we aim to build a multivariate model that predicts a brain image of an old age given a young brain.

One particular challenge is inter-subject variation: every individual has a unique ageing trajectory. Previous approaches built a spatio-temporal atlas to predict average brain images at different ages [2], [14]. However, the learnt atlas does not preserve subject-specific characteristics. Recent studies proposed subject-specific ageing progression with neural networks [3], [15], although they required longitudinal data to train. Such data are difficult and expensive to acquire, especially for longer time spans. Even in ADNI [16], the most well-known large-scale dataset, the longitudinal images are acquired at discrete time points and cover only a few years. Finding longitudinal data with a time span sufficient to simulate long-term ageing remains an open challenge.

To overcome the aforementioned challenges, we propose a deep adversarial method that learns the joint distribution of brain appearance, age and health state (AD status in this paper) without requiring longitudinal data for training. A simplified schematic of our model is illustrated in Fig. 1 along with example results. Given a brain image, our model produces a brain of the same subject at a target age and a health state. The input image is first encoded into a latent space, that is modulated by two vectors of target age difference and health state respectively. The conditioned latent space is finally decoded to an output image. The quality of synthetic results is encouraged by a discriminator that judges whether an output image is representative of the distribution of brain images of the same age and health state. A typical problem in synthesis with *cross-sectional* data [5] is loss of *subject identity*¹, i.e. the synthesis of an output that may not correspond to the

Manuscript received 4th December 2019.

Data collection and sharing for this work was funded by the Alzheimer’s Disease Neuroimaging Initiative (NIH grant U01 AG024904) and DOD ADNI (award number W81XWH-12-2-0012). This work was supported by the University of Edinburgh by PhD studentships to T. Xia and A. Chartsias. This work was supported by The Alan Turing Institute under the EPSRC grant EP/N510129/1. We thank Nvidia for donating a Titan-X GPU. S.A. Tsafaris acknowledges the support of the Royal Academy of Engineering and the Research Chairs and Senior Research Fellowships scheme.

T. Xia, A. Chartsias and S.A. Tsafaris are with the School of Engineering at the University of Edinburgh. S.A. Tsafaris is also with the Alan Turing Institute London. C. Wang is with the BHF Centre for Cardiovascular Science.

*Corresponding author, tian.xia@ed.ac.uk

¹A classical computer vision example is the synthesis of human faces with different attributes. Identity loss is an output image of a different person. Even in the analogous task of brain ageing, that of face ageing, humans still find difficult to assess identity loss.

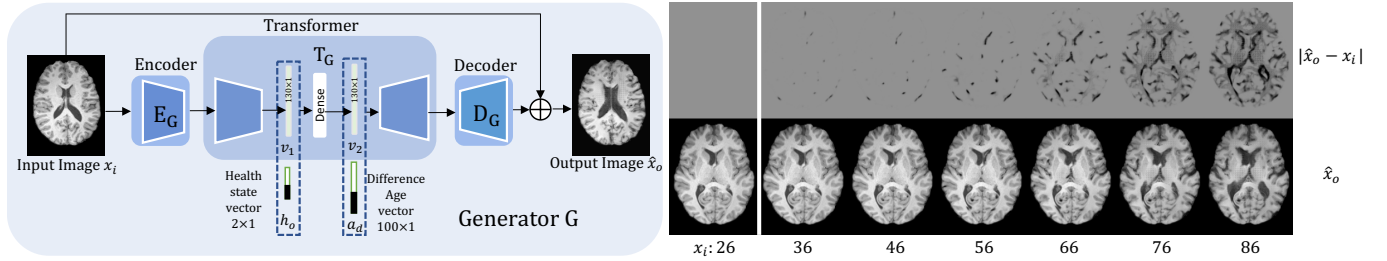


Fig. 1. **Left:** The input is a brain image x_i , and the network synthesises an aged brain image \hat{x}_o from x_i , conditioned on the target health state vector h_o and target age difference $a_d = a_o - a_i$ between input a_i and target a_o ages, respectively. **Right:** For an image x_i of a 26 year old subject, bottom row shows outputs \hat{x}_o given different target age. The top row shows the corresponding image differences $|\hat{x}_o - x_i|$ to highlight progressive changes.

input. We propose, and motivate, two loss functions that help preserve *subject identity* by essentially regularising the amount of change introduced by ageing. In addition, we motivate the design of our conditioning mechanisms and show that ordinal binary encoding for both discrete and continuous variables improves performance significantly.

We quantitatively evaluate the simulation results using longitudinal data from the ADNI dataset [16]. Since the longitudinal data only cover a limited time span, and in order to evaluate simulated images across decades, we further pre-train a VGG-network [17] to estimate the apparent age from output images. The estimated ages are used as a proxy metric for the quality of output images in terms of *age accuracy*. We also show qualitative results, including ageing simulation on different health states and long-term ageing synthesis. Both quantitative and qualitative results show that our method outperforms benchmarks with more accurate simulations that capture the characteristics specific to each individual on different health states. Furthermore, we train our model on Cam-CAN and evaluate it on ADNI to demonstrate the generalisation ability to unseen data. Finally, we perform ablation studies to investigate the effect of loss components and different ways of embedding clinical variables into the networks.

Our contributions are summarised as follows:²

- We propose a deep learning model to simulate the brain ageing process trained on *cross-sectional* data.
- Our model uses an embedding mechanism that teaches the network to learn the joint distribution of brain images, age and health state (AD status).
- We design losses that help preserve subject identity in the output images.
- We demonstrate our method’s robustness with extensive experiments on two publicly available datasets.

The manuscript proceeds as follows: Section II reviews related work on brain ageing research. Section III details the proposed method. Section IV describes the experimental setup and training details. Section V presents results and discussion. Finally, Section VI concludes the manuscript.

²We advance our preliminary work [18] in the following aspects: 1) we extend our model to condition on age and AD status, which enables more accurate simulation of ageing progression of different health states; 2) we introduce additional regularisation to smooth the simulated progression; 3) we offer more experiments and a detailed analysis of performance, using longitudinal data, including new metrics and additional benchmark methods for comparison.

II. RELATED WORK

We classify existing methods into two categories: *age-prediction* that estimate the apparent age from a brain image, and *image-simulation* that synthesise brain images conditioned on age and health state. We discuss these methods below.

Age-prediction methods: Early methods predict age using hand-crafted features with kernel regression [19] or with Gaussian Process Regression [20]. However, their performance often relies on the effectiveness of the hand-crafted features.

Recently, deep learning models have been used to estimate the brain age from imaging data. For example, [21] used a VGG-based [17] model to predict age and detect degenerative diseases, while [22] proposed to discover genetic associations with the brain degeneration using a ResNet-based network [23]. Similarly, [24] used the age predicted by a deep network to detect traumatic brain injury. However, these methods did not consider the morphological changes of brain, which is potentially more informative [25].

Image-simulation methods: Given variables such as the age, these methods aim to synthesise the corresponding brain image to enable visual observation of brain changes. For instance, patch-based dictionary learning [1] or kernel regression [2], [5], [26] was used to build spatio-temporal atlases of brains at different ages. However, these are population average atlases and thus are not able to capture brain ageing trajectories specific to each individual.

Very recently deep generative methods have been used for this task. While [15] and [27] used formulations of Generative Adversarial Networks (GAN) [28] to estimate brain changes, others [3] used conditional adversarial autoencoder, following a recent face ageing work [29], as the generative model. Irrespective of the model, these methods require longitudinal data, which limits their applicability. In [4], a GAN-based method is trained to add or remove the atrophy patterns in the brain using image arithmetics, although the atrophy patterns were modelled in a linear way and the morphological changes were assumed to be the same for all subjects. In [30], a Variational Autoencoder (VAE) was used to synthesise aged brain images, but the target age is not controlled, and the quality of the synthesised image appears poor (blurry). Similarly, [31] used a VAE to disentangle the spatial information from temporal progression, then used the first few layers of the VAE as feature extractor to improve the age prediction task. In summary, most previous methods either built atlases [1],

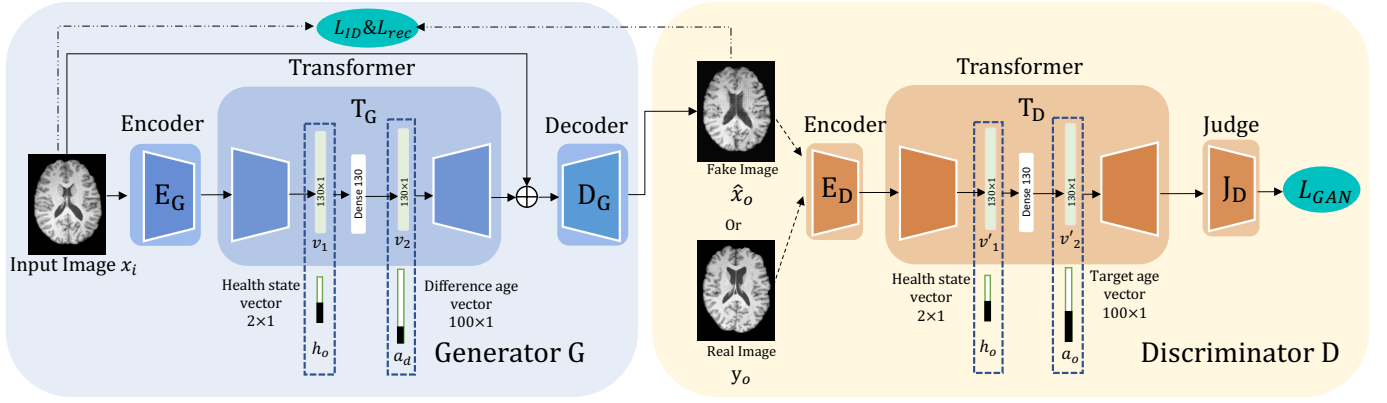


Fig. 2. An overview of the proposed method (training). x_i is the input image; h_o is the target health state; a_d is the difference between the starting age a_i and target age a_o : $a_d = a_o - a_i$; \hat{x}_o is the output (aged) image (supposedly belong to the same subject as x_i) of the target age a_o and health state h_o . The *Generator* takes as input x_i , h_o and a_d , and outputs \hat{x}_o ; the *Discriminator* takes as input a brain image and h_o and a_o , and outputs a discrimination score.

[2], [5], [26], or required longitudinal data [3], [15], [27] to simulate the brain ageing process. Other methods that did not need longitudinal data [4], [30], [31], on the other hand, produced blurry images and lost subject identity.

Our approach: To address these shortcomings, we propose a conditional adversarial training procedure that learns to simulate the brain ageing process by being *specific* to the input subject, and by learning from *cross-sectional* data without requiring longitudinal observations.

III. PROPOSED APPROACH

A. Problem statement, notation and overview

We denote a brain image as x_s (and \mathcal{X}_s their distribution such that $x_s \sim \mathcal{X}_s$), where s are the subject's clinical variables including the corresponding age a and health state (AD status) h . Given a brain image x_i of age a_i and health state h_i , we want to synthesise a brain image \hat{x}_o of target age a_o and health state h_o . Critically, the synthetic brain image \hat{x}_o should retain the subject identity, i.e. belong to the same subject as the input x_i , throughout the ageing process. The contributions of our approach, shown in Fig. 2, are the design of the conditioning mechanism; our model architecture that uses a *Generator* to synthesise images, and an adversary, a *Discriminator*, to help learn the joint distribution of clinical variables and brain appearance; and the losses we use to guide the training process. We detail all these below.

B. Conditioning on age and health state

In our previous work [18], we simulate the ageing brain with age as the single factor. Here, we extend our previous approach by involving the health state, i.e. AD status, as another factor to better simulate the ageing process.

We use ordinal binary vectors, instead of one-hot vectors as in [29], to encode both age and health state, which are embedded in the bottleneck layer of the *Generator* and *Discriminator* (detailed in Section III-C). We assume a maximal age of 100 years and use a 100×1 vector to encode age a . Similarly, we use a 2×1 vector to encode health state. A simple illustration of this encoding is shown in Fig. 3. An

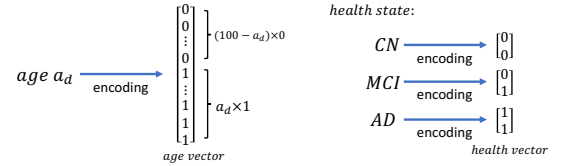


Fig. 3. Ordinal encoding of age and health state. **Left** shows how we represent age a_d using a binary vector with first a_d elements as 1 and the rest as 0; **Right** is the encoding of health state, where we use a 2×1 vector to represent three categories of AD status from CN (healthy) to AD.

ablation study presented in Section V-C illustrates the benefits of *ordinal* v.s. *one-hot* encoding.

C. Proposed model

The proposed method consists of a *Generator* and a *Discriminator*. The *Generator* synthesises aged brain images corresponding to a target age and a health state. The *Discriminator* has a dual role: firstly, it discriminates between ground-truth and synthetic brain images; secondly, it ensures that the synthetic brain images correspond to the target clinical variables. The *Generator* is adversarially trained to generate realistic brain images of the correct target age. The detailed network architectures are shown in Fig. 4.

1) *Generator*: The *Generator* G takes as input a 2D brain image x_i , and ordinal binary vectors for target health state h_o and age difference a_d . Here, we condition on the age difference between input age a_i and target age a_o : $a_d = a_o - a_i$, such that when input and output ages are equal $a_d = 0$, the network is encouraged to recreate the input. The output of G is a 2D brain image \hat{x}_o corresponding to the target age and health state.³

G has three components: the *Encoder* E_G , the *Transformer* T_G and the *Decoder* D_G . E_G first extracts latent features from the input image x_i . T_G involves the target age and health state into the network. Finally, D_G generates the aged brain image from the bottleneck features. To embed age and health state into our model, we first concatenate the latent

³Note that the target health state can be different from the corresponding input state. This encourages learning a joint distribution between brain images and clinical variables.

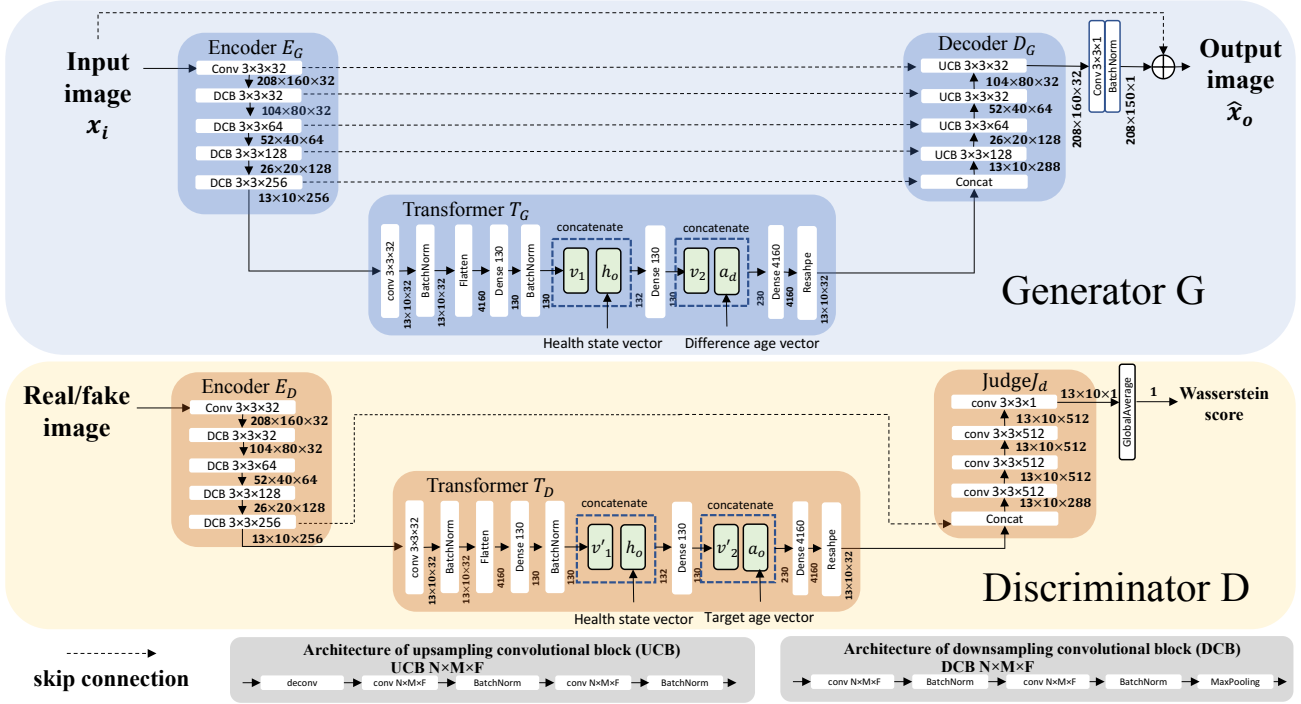


Fig. 4. Detailed architectures of *Generator* and *Discriminator*. The Generator contains three parts: an Encoder to extract latent features; a Transformer to involve target age and health state; and a Decoder to generate aged images. Similarly, we use the same conditioning mechanism for the Discriminator to inject the information of age and health state, and a long skip connection to better preserve features of input image.

vector v_1 , obtained by E_G , with the health state vector h_o . The concatenated vector is then processed by a dense layer to output latent vector v_2 , which is then concatenated with the difference age vector a_d . Finally, the resulting vector is used to generate the output image.⁴ We adopt long-skip connections [32] between layers of E_G and D_G to preserve details of the input image and improve the sharpness of the output images. Overall, the Generator’s forward pass is: $\hat{x}_o = G(x_i, a_d, h_o)$.

2) *Discriminator*: Similar to the Generator, the Discriminator D contains three subnetworks: the *Encoder* E_D that extracts latent features, the *Transformer* T_D that involves the conditional variables, and the *Judge* J_D that outputs a discrimination score.

Note that D is conditioned on the target age a_o instead of age difference a_d , to learn the joint distribution of brain appearance and age, such that it can discriminate between real and synthetic images of correct age. The forward pass for the Discriminator is $w_{fake} = D(\hat{x}_o, a_o, h_o)$ and $w_{real} = D(y_o, a_o, h_o)$.

D. Losses

We train with a multi-component loss function containing *adversarial*, *identity-preservation* and *self-reconstruction* losses. We detail these below.

⁴We tested the ordering of h_o and a_d , and it did not affect the results. We also tried to concatenate h_o , a_d and v_1 together into one vector, and use the resulting vector to generate the output. However, we found that the model tended to ignore the information of h_o . This might be caused by the dimensional imbalance between h_o (2×1) and a_d (100×1).

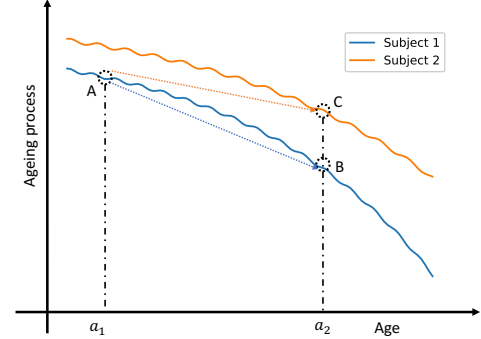


Fig. 5. Illustration of ageing trajectories for two subjects. For a subject of age a_1 (A), the network can learn a mapping from A to C, which could still fool the Discriminator, but loses the identity of Subject 1 (orange line).

1) *Adversarial loss*: We adopt the Wasserstein loss with gradient penalty [33] to predict a realistic aged brain image \hat{x}_o and force the aged brain to correspond to the target age a_o and health state h_o :

$$L_{GAN} = \min_{\mathbf{G}} \max_{\mathbf{D}} \mathbb{E}_{y_o \sim \mathcal{X}_o, \hat{x}_o \sim \hat{\mathcal{X}}_o} [D(y_o, a_o, h_o) - D(\hat{x}_o, a_o, h_o) + \lambda_{GP} (\|\nabla_{\tilde{z}} D(\tilde{z}, a_o, h_o)\|_2 - 1)_2], \quad (1)$$

where \hat{x}_o is the output image: $\hat{x}_o = G(x_i, a_d, h_o)$ ($a_d = a_o - a_i$), y_o is a ground truth image from another subject of target age a_o and health state h_o , \tilde{z} is the average sample defined by $\tilde{z} = \epsilon \hat{x}_o + (1 - \epsilon)y_o$, $\epsilon \sim U[0, 1]$. The first two terms measure the Wasserstein distance between ground-truth and synthetic samples; the last term is the gradient penalty involved to stabilise training. As in [33], [34] we set $\lambda_{GP} = 10$.

2) *Identity-preservation loss*: While L_{GAN} encourages the network to synthesise realistic brain images, these images may lose subject identity. For example, it is easy for the network to learn a mapping to an image that corresponds to the target age and health state, but belongs to a different subject. An illustration is presented in Fig. 5, where ageing trajectories of two subjects are shown. The task is to predict the brain image of subject 1 at age a_2 starting at age a_1 , by learning a mapping from point A to point B. But there are no ground-truth data to ensure that we stay on the trajectory of subject 1. Instead, the training data contain brain images of age a_2 belonging to subject 2 (and other subjects). Using only L_{GAN} , the Generator may learn a mapping from A to C to fool the Discriminator, which will lose the identity of subject 1. In order to alleviate this and encourage the network to learn mappings along trajectory (i.e. from A to B), we adopt:

$$L_{ID} = \min_G \mathbb{E}_{x_i \sim \mathcal{X}_i, \hat{x}_o \sim \mathcal{X}_o} \|x_i - \hat{x}_o\|_1 \cdot e^{-\frac{|a_o - a_i|}{|a_{max} - a_{min}|}}, \quad (2)$$

where x_i is the input image of age a_i and \hat{x}_o is the output image of age a_o ($a_o > a_i$). The term $e^{-\frac{|a_o - a_i|}{|a_{max} - a_{min}|}}$ encourages that $\|x_i - \hat{x}_o\|_1$ should positively correlate with the difference between a_o and a_i . Note that the health state is not involved in L_{ID} . The exponential term does not aim to precisely model the ageing trajectory. Instead, it is used to encourage identity preservation by penalising heavy transformations between close ages, and also stabilise training. A more accurate ageing prediction, that is also correlated with the health state, is achieved by the adversarial learning. An ablation study illustrating the critical role of L_{ID} is presented in Section V-C.

3) *Self-reconstruction loss*: When the target age and health state are the same as the input, the Generator should reconstruct the input image. We use a self-reconstruction loss to explicitly encourage this input reconstruction:

$$L_{rec} = \min_G \mathbb{E}_{x_i \sim \mathcal{X}_i, \hat{x}_i \sim \mathcal{X}_i} \|x_i - \hat{x}_i\|_1, \quad (3)$$

where x_i and \hat{x}_i are the input and output images respectively, of the same age and health state. Although L_{rec} is similar to L_{ID} , their roles are different: L_{ID} helps to preserve subject identity when generating aged images, while L_{rec} encourages the simulation of a smooth progression via self-reconstruction. An ablation study on L_{rec} in Section V-C shows the importance of stronger regularisation.⁵

IV. EXPERIMENTAL SETUP

Datasets: We use two datasets, as detailed below.

Cambridge Centre for Ageing and Neuroscience (Cam-CAN) [35] is a cross-sectional dataset containing normal subjects aged 17 to 85. To improve age distribution, we discarded subjects under 25 or over 85 years old. We split subjects into different age groups spanning 5 years. We randomly selected 38 volumes from each group and used 30 for training and 8

for testing. We use Cam-CAN to demonstrate consistent brain age synthesis across the whole lifespan.

Alzheimer’s Disease Neuroimaging Initiative (ADNI) [16] is a longitudinal dataset, which contains cognitively normal (CN) subjects, subjects with mild cognitive impairment (MCI) and subjects with AD. We use ADNI to demonstrate brain image synthesis, conditioned on different health states. Since ADNI has longitudinal data, we used these data to quantitatively evaluate the quality of synthetically aged images. We chose 786 subjects as training (279 CN, 260 MCI, 247 AD), and 136 subjects as testing data (49 CN, 46 MCI, 41 AD).

Pre-processing: All volumetric data are skull-stripped using DeepBrain⁶, and linearly registered to MNI 152 space using FSL-FLIRT [36]. We normalise brain volumes by clipping the intensities to $[0, V_{99.5}]$, where $V_{99.5}$ is the 99.5% largest intensity value within each volume, and then rescale the resulting intensities to the range $[-1, +1]$. We select the middle 60 axial slices from each volume, and crop each slice to the size of $[208, 160]$. During training, we only use *cross-sectional* data, i.e. one subject only has one volume of a certain age. During testing, we use the longitudinal ADNI data covering more than 2 years, and discard data where images are severely misaligned due to registration errors.

Benchmarks: We compare with the following benchmarks⁷:

Conditional GAN: This approach from image translation [37], estimates an output conditioned on the input. To make it comparable with our method, we train different Conditional GANs for transforming young images to different older age groups. Therefore, a single model of ours is compared with age-group specific Conditional GANs.

CycleGAN: We compare with CycleGAN [38], where there are two translation paths: from ‘young’ to ‘old’ to ‘young’, and from ‘old’ to ‘young’ to ‘old’. Similarly to Conditional GAN, we train several CycleGANs for different target age groups.

CAAE: We compare with [29], a recent paper for face ageing synthesis. We use the official implementation⁸, modified to fit our input image shape. This method used a Conditional Adversarial Autoencoder (CAAE) to perform face ageing synthesis by concatenating a one-hot age vector with the bottleneck vector. They divided age into discrete categories with each category containing one age group.

Implementation details: The overall training loss is:

$$L = \lambda_1 L_{GAN} + \lambda_2 L_{ID} + \lambda_3 L_{rec}, \quad (4)$$

where $\lambda_1 = 1$, $\lambda_2 = 100$ and $\lambda_3 = 10$ are hyper-parameters used to balance each loss. The λ parameters are chosen experimentally. We chose λ_2 as 100 following [18], [34], and λ_3 as a smaller value 10 as we focus more on brain ageing synthesis rather than reconstruction.

During training, we divide subjects into a young group and an old group, and randomly draw a young sample x_i and an old sample y_o to synthesise the aged image \hat{x}_o of target age a_o and

⁶<https://github.com/iitzco/deepbrain>

⁵In our previous work [18], Eq. 2 did not have the $a_o > a_i$ constraint and might randomly include the case of $a_o = a_i$ to encourage self-reconstruction. However, as shown in Section V-C, stronger regularisation is necessary.

⁷We also experimented with the official implementation of [30] however our experiments confirmed the poor image quality reported by the author.

⁸<https://zzutk.github.io/Face-ageing-CAAE/>

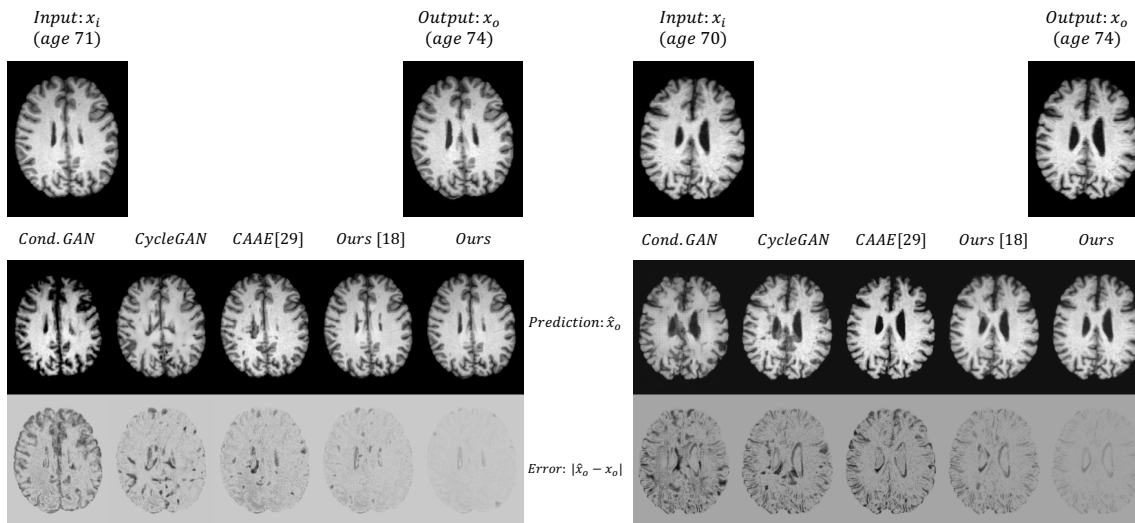


Fig. 6. Example results of subjects with ground-truth follow-up studies. We predict output \hat{x}_o from input x_i using benchmarks and our method. We also show errors between the outputs and the ground-truths as $|\hat{x}_o - x_o|$. We can observe that our method achieves the most accurate results outperforming our previous method [18] and benchmarks. For more details see text.

health state h_o . Note that $a_o > a_i$, and h_o could be different than h_i . We train all methods for 600 epochs. We update the generator and discriminator in an iterative fashion [28], [39]. Since the discriminator in Wasserstein GAN needs to be close to optimal during training, we updated the discriminator for 5 iterations per generator update. Initially, for the first 20 epochs, we updated the discriminators for 50 iterations per generator update. We use Keras [40] and train with Adam [41] with a learning rate of 0.0001 and decay of 0.0001. Code will be made publicly available at <https://upon.acceptance>.

Evaluation metrics: To evaluate the quality of synthetically aged images, we first use the longitudinal data from ADNI dataset. We select follow-up studies that cover more than 2 years to allow observable neurodegenerative changes to happen. We used standard definitions of *mean squared error* (MSE), *peak signal-to-noise ratio* (PSNR) and *structural similarity* (SSIM) of window length of 11 [42] to evaluate the closeness of the predicted images to the ground-truth.

However, longitudinal data in ADNI only cover a short time span. Therefore, we also propose a proxy metric to evaluate the output images. We first pre-train a VGG-like [17] network to predict age from brain images, then use this age predictor, f_{pred} , to estimate the apparent age of output images. The difference between the predicted and desired target age is then used to evaluate how close the generated images are to the target age. Formally, we define *predicted age difference* (PAD): $PAD = \mathbb{E}_{\hat{x}_o \sim x_o} |f_{pred}(\hat{x}_o) - a_o|$. The age predictor f_{pred} is pre-trained on Cam-CAN and healthy (CN) ADNI training data, and achieves an average testing error of 5.1 years.

Statistics: All results are obtained on testing sets. We use **bold** font to denote the best performing method (for each metric) and an asterisk (*) to denote statistical significance. We use a paired t-test (at 5% level assessed via permutations) to test the null hypothesis that there is no difference between our methods and the best performing benchmark.

V. RESULTS AND DISCUSSION

We start our experiments showing quantitative and qualitative results on ADNI and then Cam-CAN. We then conclude with several ablation studies to illustrate the importance of each component in our model.

A. Brain ageing synthesis on different health states (ADNI)

In this section, we train and evaluate our model on ADNI dataset, which contains CN, MCI and AD subjects. Our model is trained only on *cross-sectional* data. The results and discussions are detailed below.

1) *Quantitative results:* The quantitative results are shown in Table I employing the metrics defined in Section IV. We can observe that our method achieves the best results in all metrics, with second best being the previous (more simple incarnation) [18] of the proposed model. Clearly, embedding health state improves performance. The third best results are achieved by CAAE [29], where age is divided into 10 categories and represented by a one-hot vector. To generate the aged images at the target age (the age of the follow-up studies), we use the category which the target age belongs to, i.e. if the target age is 76, then we choose the category of age 75-78. We see the benefits of encoding age into ordinal vectors, where the difference between two vectors positively correlates with the difference between two ages in a finely-grained fashion. CycleGAN and Conditional GAN achieve the poorest results

TABLE I
QUANTITATIVE EVALUATION ON ADNI DATASET.

	SSIM	PSNR	MSE	PAD
Cond. GAN	0.39±0.08	14.2±3.5	0.202±0.012	9.5±4.7
CycleGAN	0.46±0.07	16.3±3.3	0.193±0.008	9.7±5.1
CAAE [29]	0.64±0.07	20.3±2.9	0.114±0.011	5.4±4.5
Ours [18]	0.73±0.06	23.3±2.2	0.081±0.009	5.0±3.7
Ours	0.79±0.06	26.1±2.6	0.042±0.006	4.2±3.9

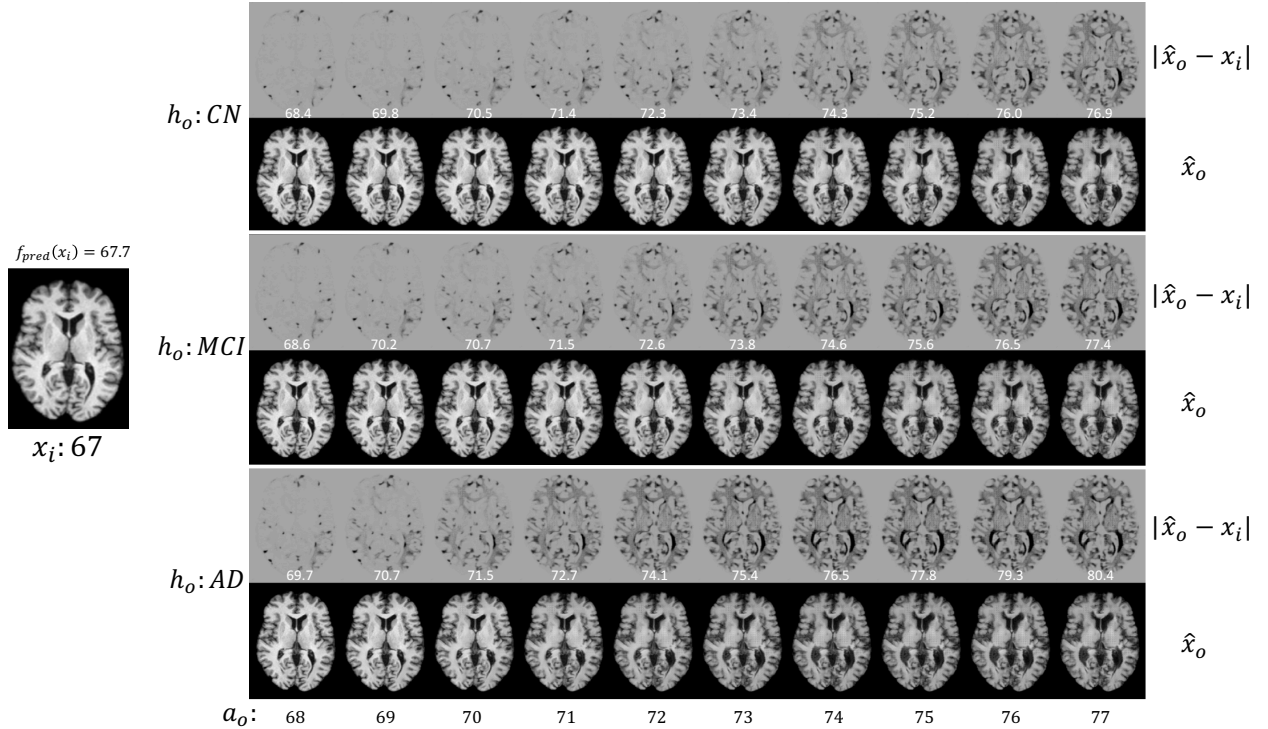


Fig. 7. Brain ageing progression for one healthy (CN) subject x_i (at age 70) from ADNI dataset. We synthesise the aged images \hat{x}_o at different target ages a_o on different health states h_o : CN, MCI and AD, respectively. We also visualise the difference between x_i and \hat{x}_o , $|\hat{x}_o - x_i|$, and show the predicted ages of \hat{x}_o by our pre-trained age predictor (white text on top of each brain). For more details see text.

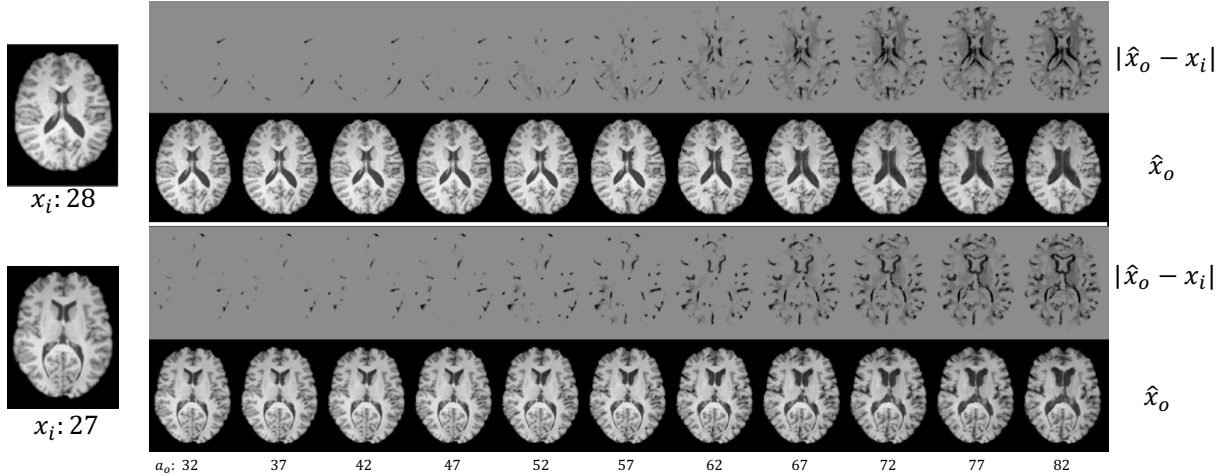


Fig. 8. Long-term brain ageing synthesis on Cam-CAN dataset. We synthesise the aged images \hat{x}_o at different target ages a_o and show the difference between input images x_i and \hat{x}_o , $|\hat{x}_o - x_i|$. For more details see text.

unsurprisingly, since conditioning here happens explicitly by training separate models according to different age groups.

2) *Qualitative results*: Visual examples on two images from ADNI, are shown in Fig. 6. For both examples, our method generates most accurate predictions, followed by our previous method, offering visual evidence to the observations above. The third best results are achieved by CAEE, where we can see more errors between prediction \hat{x}_o and ground-truth x_o . CycleGAN and Conditional GAN produced the poorest output images, with observable structural differences from ground-truth, which indicates the loss of subject identity.

Furthermore, we demonstrate visual results of the same subject on different target health states h_o , as shown in Fig. 7. We can observe that for all h_o , the brain changes gradually as a_o increases. However, the ageing rate is different on different health states. Specifically, when h_o is CN, the ageing rate is slower than that of MCI and AD; when h_o is AD, the ageing process achieved the fastest rate. We also report the estimated ages of these synthetic images by f_{pred} . The results show that the predicted ages on AD are ‘older’ than the target ages and those on CN and MCI, which is consistent with the fact that AD accelerates brain ageing [16].

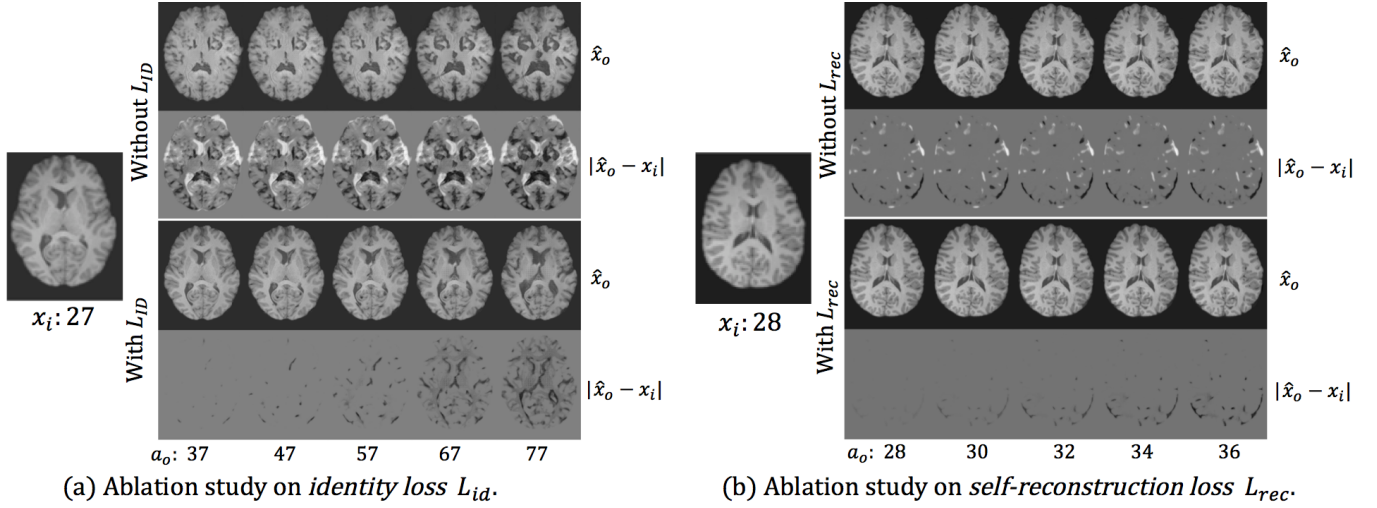


Fig. 9. Ablation studies for loss components. **Left:** ablation study of L_{ID} . Top row shows that without L_{ID} , the network can lose the subject identity. Bottom row shows that the use of L_{ID} can enforce the preservation of subject identity, such that the changes as ages are smooth and consistent. **Right:** ablation study on L_{rec} . When L_{rec} is not used (top two rows), there are sudden changes at the beginning of ageing progression simulation (even at the original age), which hinders the preservation of subject identity. In contrast, when L_{rec} is used (bottom two rows), the ageing progression is smoother, which demonstrates better identity preservation.

B. Long term brain ageing synthesis

Here we apply our model on Cam-CAN dataset where no longitudinal data are available. The qualitative and quantitative results are detailed below.

1) *Qualitative results:* In Fig. 8, we demonstrate the simulated brain ageing process throughout the whole lifespan, where the input images are two young subjects from Cam-CAN dataset. We observe that the output images gradually change as a_o increases, with ventricular enlargement and brain tissue reduction. This change pattern is consistent with previous studies [43], [44], implying that our method learns to consistently synthesise the ageing brain throughout lifespan even trained on *cross-sectional* data.

2) *Quantitative results (generalisation performance on ADNI):* Cam-CAN is a *cross-sectional* dataset. To quantitatively evaluate the quality of synthetic images, we use the longitudinal portion of ADNI data, and specifically only the CN cohort, to demonstrate the generalisation performance. The results are shown in Table II. We observe that though our model is trained and evaluated on different datasets, it still achieves comparable results with those of Table I and outperforms benchmarks. This indicates the generalisation ability of our model to unseen data.

TABLE II
QUANTITATIVE EVALUATION OF METHODS TRAINED ON CAM-CAN AND EVALUATED ON ADNI.

	SSIM	PSNR	MSE	PAD
Cond. GAN	0.38 ± 0.12	13.9 ± 4.2	0.221 ± 0.021	11.3 ± 5.6
CycleGAN	0.42 ± 0.09	14.4 ± 3.8	0.212 ± 0.016	10.2 ± 5.5
CAAE [29]	0.59 ± 0.10	19.3 ± 3.9	0.121 ± 0.012	5.9 ± 4.7
Ours [18]	0.68 ± 0.08	22.7 ± 2.8	0.095 ± 0.014	5.3 ± 3.8
Ours	0.74 ± 0.08	24.2 ± 2.7	0.043 ± 0.009	5.0 ± 3.6

C. Ablation studies

We perform ablation studies on loss components and embedding mechanisms to inject clinical variables into networks.

1) *Effect of loss components:* We demonstrate the effect of L_{ID} and L_{rec} by assessing the model performance when each component is removed. In Table III we show quantitative results on ADNI dataset. In Fig. 9 we illustrate qualitative results on Cam-CAN dataset to visualise the effect. We can observe that the best results are achieved when all loss components are used. Specifically, without L_{ID} , the synthetic images lost subject identity severely throughout the whole progression, i.e. the output image appears to come from a different subject; without L_{rec} , output images suffer from sudden changes at the beginning of progression, even when $a_o = a_i$. Both quantitative and qualitative results show that the design of L_{ID} and L_{rec} improves preservation of subject identity and enables more accurate brain ageing simulation.

2) *Effect of different embedding mechanisms:* We investigate the effect of different embedding mechanisms. Our embedding mechanism is described in Section III. Here, we first perform experiments where we use *one-hot* v.s. *ordinal* vectors to encode age and health state. The qualitative results are shown in Fig. 10. We can see when we use *one-hot* vectors to encode age and health state, the network still generates realistic images, but the ageing progression is not consistent, i.e. synthetic brains appear to have ventricle enlarging or

TABLE III
QUANTITATIVE EVALUATION WHEN TRAINING WITH DIFFERENT COMBINATIONS OF COST FUNCTIONS.

	SSIM	PSNR	MSE
L_{GAN}	0.55 ± 0.14	18.4 ± 3.7	0.132 ± 0.013
$L_{GAN} + L_{rec}$	0.62 ± 0.12	19.6 ± 3.2	0.089 ± 0.014
$L_{GAN} + L_{ID}$	0.74 ± 0.07	24.3 ± 2.5	0.074 ± 0.010
$L_{GAN} + L_{ID} + L_{rec}$	0.79 ± 0.08	26.1 ± 2.6	0.042 ± 0.006

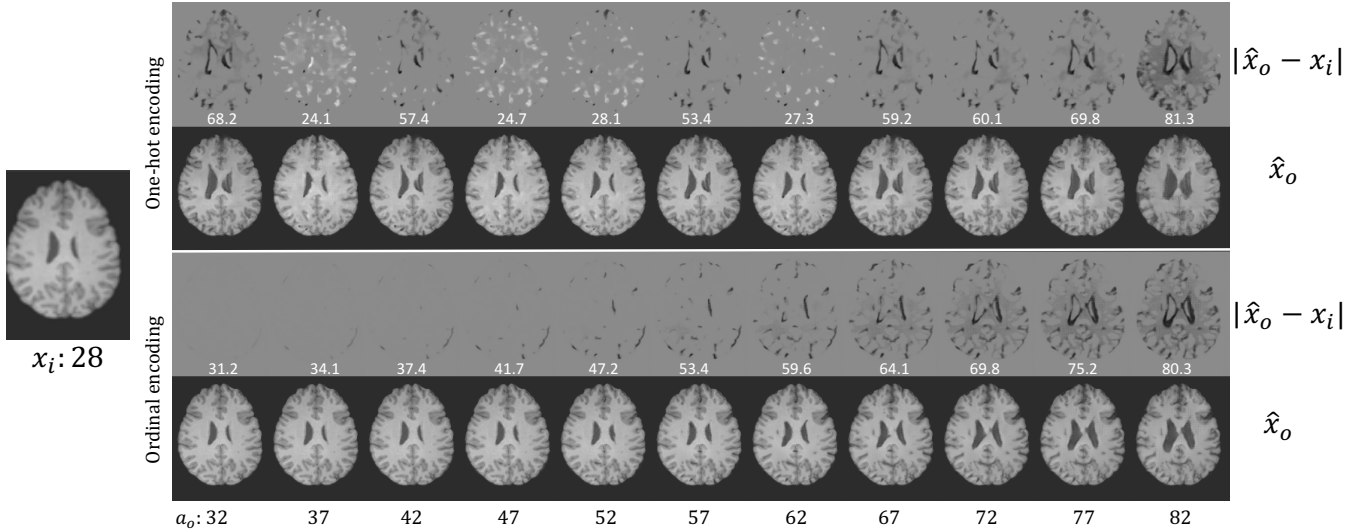


Fig. 10. Example results for *one-hot* v.s. *ordinal encoding* on Cam-CAN dataset. We synthesise aged images \hat{x}_o at different target ages a_o with *one-hot encoding* v.s. *ordinal encoding*. We also visualise the difference between input image x_i and \hat{x}_o , $|\hat{x}_o - x_i|$, and we report the estimated age of these images by the pre-trained age predictor (shown as white text on top of each brain).

TABLE IV
QUANTITATIVE RESULTS OF DIFFERENT EMBEDDING MECHANISMS.

	SSIM	PSNR	MSE	PAD
One-hot	0.54 ± 0.14	17.3 ± 3.8	0.177 ± 0.014	9.7 ± 4.9
concat _{all}	0.74 ± 0.09	23.9 ± 2.9	0.065 ± 0.011	5.2 ± 3.9
Ours	$0.79^* \pm 0.08$	$26.1^* \pm 2.6$	$0.042^* \pm 0.006$	5.0 ± 3.6

shrinking in random fashion across age. In contrast, with *ordinal encoding*, the model simulates the ageing process consistently. This observation is confirmed by the estimated ages of the output images by f_{pred} .

We also compare with an embedding strategy where we concatenate h_o , a_d and the bottleneck latent vector v_1 together, and the concatenated vector is processed by the Decoder to generate the output image. We refer to this embedding strategy as *concat_{all}*. We found with *concat_{all}*, the network tends to ignore the health state vector h_o and only use the information of a_d . This can be caused by the dimensional imbalance between h_o (2×1) and a_d (100×1). The quantitative results on ADNI are shown in Table IV. We can see that when *one-hot encoding* is used, the results dropped significantly, followed by *concat_{all}*, confirming our observation.

VI. CONCLUSION

We present a method that learns to simulate subject-specific aged images *without* longitudinal data. Our method relies on a Generator to generate the images and a Discriminator that captures the joint distribution of brain images and clinical variables, i.e. age and health state (AD status). We propose an embedding mechanism to encode the information of age and health state into our network, and age-modulated and self-reconstruction losses to preserve *subject identity*. We present qualitative results showing that our method is able to generate consistent and realistic images conditioned on the target age and health state. We evaluate with longitudinal data from

ADNI and a proposed numerical evaluation metric for *age accuracy*. We demonstrate on ADNI and Cam-CAN datasets that our model outperforms benchmarks both qualitatively and quantitatively and via a series of ablations illustrate the importance of each design decision.

We see several avenues for future improvements by us or the community. Conditioning mechanisms that reliably embed prior information into neural networks enabling finer control over the outputs of models are of considerable interest in deep learning. In this paper we design a simple, yet effective, way to encode both *age* (continuous) and *AD status* (ordinal) factors into the image generation network. However, incorporating additional clinical variables, e.g. gender, genotypes, education, etc., could be inefficient with our current approach as it may involve more dense layers. While new techniques are available [45]–[48] and some prior examples on few conditioning variables [49] or disentanglement [50] are promising, their utility in integrating clinical variables with imaging data is under investigation. Although we used brain data, the approach could be extended to other organs or estimating the future state of pathology. Finally, despite our efforts to introduce 3D networks, this work remains 2D: the parameter space exploded due to the size of 3D networks.

REFERENCES

- [1] Y. Zhang, F. Shi, G. Wu, L. Wang, P.-T. Yap, and D. Shen, “Consistent spatial-temporal longitudinal atlas construction for developing infant brains,” *TMI*, vol. 35, no. 12, pp. 2568–2577, 2016.
- [2] W. Huizinga, D. H. Poot, M. W. Vernooij, G. Roshchupkin, E. Bron, M. A. Ikram, D. Rueckert, W. J. Niessen, S. Klein, A. D. N. Initiative *et al.*, “A spatio-temporal reference model of the aging brain,” *NeuroImage*, vol. 169, pp. 11–22, 2018.
- [3] D. Ravi, D. C. Alexander, and N. P. Oxtoby, “Degenerative Adversarial NeuroImage Nets: Generating Images that Mimic Disease Progression,” *MICCAI*, 2019.
- [4] C. Bowles, R. Gunn, A. Hammers, and D. Rueckert, “Modelling the progression of Alzheimer’s disease in MRI using generative adversarial networks,” in *Medical Imaging 2018: Image Processing*, 2018.

- [5] G. Ziegler, R. Dahnke, and C. Gaser, "Models of the aging brain structure and individual decline," *Frontiers in Neuroinformatics*, vol. 6, p. 3, 2012.
- [6] L. Zecca, M. B. Youdim, P. Riederer, J. R. Connor, and R. R. Crichton, "Iron, brain ageing and neurodegenerative disorders," *Nature Reviews Neuroscience*, vol. 5, no. 11, p. 863, 2004.
- [7] M. P. Mattson and T. V. Arumugam, "Hallmarks of brain aging: adaptive and pathological modification by metabolic states," *Cell Metabolism*, vol. 27, no. 6, pp. 1176–1199, 2018.
- [8] C. López-Otín, M. A. Blasco, L. Partridge, M. Serrano, and G. Kroemer, "The hallmarks of aging," *Cell*, vol. 153, no. 6, pp. 1194–1217, 2013.
- [9] J. H. Cole, R. E. Marioni, S. E. Harris, and I. J. Deary, "Brain age and other bodily ages: implications for neuropsychiatry," *Molecular Psychiatry*, vol. 24, no. 2, p. 266, 2019.
- [10] A. M. Fjell and K. B. Walhovd, "Structural brain changes in aging: courses, causes and cognitive consequences," *Reviews in the Neurosciences*, vol. 21, no. 3, pp. 187–222, 2010.
- [11] C. Jack, R. C. Petersen, Y. Xu, P. C. O'Brien, G. E. Smith, R. J. Ivnik, E. G. Tangalos, and E. Kokmen, "Rate of medial temporal lobe atrophy in typical aging and Alzheimer's disease," *Neurology*, vol. 51, no. 4, pp. 993–999, 1998.
- [12] L. G. Coleman Jr, W. Liu, I. Oguz, M. Styner, and F. T. Crews, "Adolescent binge ethanol treatment alters adult brain regional volumes, cortical extracellular matrix protein and behavioral flexibility," *Pharmacology Biochemistry and Behavior*, vol. 116, pp. 142–151, 2014.
- [13] M. Taubert, B. Draganski, A. Anwander, K. Müller, A. Horstmann, A. Villringer, and P. Ragert, "Dynamic properties of human brain structure: learning-related changes in cortical areas and associated fiber connections," *Journal of Neuroscience*, vol. 30, no. 35, pp. 11670–11677, 2010.
- [14] B. C. Davis, P. T. Fletcher, E. Bullitt, and S. Joshi, "Population shape regression from random design data," *IJCV*, vol. 90, no. 2, pp. 255–266, 2010.
- [15] M. F. Rachmadi, M. d. C. Valdés-Hernández, S. Makin, J. M. Wardlaw, and T. Komura, "Predicting the Evolution of White Matter Hyperintensities in Brain MRI using Generative Adversarial Networks and Irregularity Map," *MICCAI*, 2019.
- [16] R. C. Petersen, P. Aisen, L. A. Beckett, M. Donohue, A. Gamst, D. J. Harvey, C. Jack, W. Jagust, L. Shaw, A. Toga *et al.*, "Alzheimer's disease neuroimaging initiative (ADNI): clinical characterization," *Neurology*, vol. 74, no. 3, pp. 201–209, 2010.
- [17] K. Simonyan and A. Zisserman, "Very deep convolutional networks for large-scale image recognition," in *ICLR*, 2015.
- [18] Xia, Tian and Chatsias, Agisilaos and Tsaftaris, Sotirios A and Alzheimers Disease Neuroimaging Initiative and others, "Consistent brain ageing synthesis," in *MICCAI*. Springer, 2019, pp. 750–758.
- [19] Franke, Katja and Ziegler, Gabriel and Klöppel, Stefan and Gaser, Christian and Alzheimer's Disease Neuroimaging Initiative and others, "Estimating the age of healthy subjects from T1-weighted MRI scans using kernel methods: exploring the influence of various parameters," *Neuroimage*, vol. 50, no. 3, pp. 883–892, 2010.
- [20] J. H. Cole and K. Franke, "Predicting age using neuroimaging: innovative brain ageing biomarkers," *Trends in Neurosciences*, vol. 40, no. 12, pp. 681–690, 2017.
- [21] J. H. Cole, S. J. Ritchie, M. E. Bastin, M. V. Hernández, S. M. Maniega, N. Royle, J. Corley, A. Pattie, S. E. Harris, Q. Zhang *et al.*, "Brain age predicts mortality," *Molecular Psychiatry*, 2017.
- [22] B. Jonsson, G. Bjornsdottir, T. Thorgeirsson, L. Ellingsen, G. B. Walters, D. Gudbjartsson, H. Stefansson, K. Stefansson, and M. Ulfarsson, "Deep learning based brain age prediction uncovers associated sequence variants," *bioRxiv*, p. 595801, 2019.
- [23] K. He, X. Zhang, S. Ren, and J. Sun, "Deep residual learning for image recognition," in *CVPR*, 2016.
- [24] Cole, James H and Leech, Robert and Sharp, David J and Alzheimer's Disease Neuroimaging Initiative, "Prediction of brain age suggests accelerated atrophy after traumatic brain injury," *Annals of Neurology*, vol. 77, no. 4, pp. 571–581, 2015.
- [25] S. G. Costafreda, I. D. Dinov, Z. Tu, Y. Shi, C.-Y. Liu, I. Kloszewska, P. Mecocci, H. Soininen, M. Tsolaki, B. Vellas *et al.*, "Automated hippocampal shape analysis predicts the onset of dementia in mild cognitive impairment," *Neuroimage*, vol. 56, no. 1, pp. 212–219, 2011.
- [26] A. Serag, P. Aljabar, G. Ball, S. J. Counsell, J. P. Boardman, M. A. Rutherford, A. D. Edwards, J. V. Hajnal, and D. Rueckert, "Construction of a consistent high-definition spatio-temporal atlas of the developing brain using adaptive kernel regression," *NeuroImage*, vol. 59, no. 3, pp. 2255–2265, 2012.
- [27] V. Wegmayr, M. Hörold, and J. M. Buhmann, "Generative Aging of Brain MR-Images and Prediction of Alzheimer Progression," in *German Conference on Pattern Recognition*. Springer, 2019, pp. 247–260.
- [28] I. Goodfellow, J. Pouget-Abadie, M. Mirza, B. Xu, D. Warde-Farley, S. Ozair, A. Courville, and Y. Bengio, "Generative adversarial nets," in *NeurIPS*, 2014, pp. 2672–2680.
- [29] Z. Zhang, Y. Song, and H. Qi, "Age progression/regression by conditional adversarial autoencoder," in *CVPR*, 2017, pp. 5810–5818.
- [30] D. Milana, "Deep generative models for predicting Alzheimer's disease progression from MR data," Master's thesis, Politecnico Di Milano, 2017.
- [31] Q. Zhao, E. Adeli, N. Honnorat, T. Leng, and K. M. Pohl, "Variational autoencoder for regression: Application to brain aging analysis," *arXiv preprint arXiv:1904.05948*, 2019.
- [32] O. Ronneberger, P. Fischer, and T. Brox, "U-net: Convolutional networks for biomedical image segmentation," in *International Conference on Medical image computing and computer-assisted intervention*. Springer, 2015, pp. 234–241.
- [33] I. Gulrajani, F. Ahmed, M. Arjovsky, V. Dumoulin, and A. C. Courville, "Improved training of Wasserstein GANs," in *NeurIPS*, 2017, pp. 5767–5777.
- [34] C. F. Baumgartner, L. M. Koch, K. Can Tezcan, J. Xi Ang, and E. Konukoglu, "Visual feature attribution using wasserstein GANs," in *CVPR*, 2018, pp. 8309–19.
- [35] J. R. Taylor, N. Williams, R. Cusack, T. Auer, M. A. Shafto, M. Dixon, L. K. Tyler, and R. N. Henson, "The Cambridge Centre for Ageing and Neuroscience (Cam-CAN) data repository: Structural and functional MRI, MEG, and cognitive data from a cross-sectional adult lifespan sample," *NeuroImage*, vol. 144, pp. 262–9, 2017.
- [36] M. W. Woolrich, S. Jbabdi, B. Patenaude, M. Chappell, S. Makni, T. Behrens, C. Beckmann, M. Jenkinson, and S. M. Smith, "Bayesian analysis of neuroimaging data in FSL," *Neuroimage*, vol. 45, no. 1, pp. S173–S186, 2009.
- [37] M. Mirza and S. Osindero, "Conditional generative adversarial nets," *arXiv preprint arXiv:1411.1784*, 2014.
- [38] J.-Y. Zhu, T. Park, P. Isola, and A. A. Efros, "Unpaired image-to-image translation using cycle-consistent adversarial networks," in *Proceedings of the IEEE international conference on computer vision*, 2017, pp. 2223–2232.
- [39] M. Arjovsky, S. Chintala, and L. Bottou, "Wasserstein generative adversarial networks," in *ICML*, 2017.
- [40] F. Chollet *et al.*, "Keras," <https://keras.io>, 2015.
- [41] D. P. Kingma and J. Ba, "Adam: A method for stochastic optimization," *International Conference on Learning Representations*, 2015.
- [42] Z. Wang, E. P. Simoncelli, and A. C. Bovik, "Multiscale structural similarity for image quality assessment," in *The Thirty-Seventh Asilomar Conference on Signals, Systems & Computers, 2003*, vol. 2. IEEE, 2003, pp. 1398–1402.
- [43] C. D. Good, I. S. Johnsrude, J. Ashburner, R. N. Henson, K. J. Friston, and R. S. Frackowiak, "A voxel-based morphometric study of ageing in 465 normal adult human brains," *Neuroimage*, vol. 14, no. 1, pp. 21–36, 2001.
- [44] D. Mitchen and C. Gaser, "Computational morphometry for detecting changes in brain structure due to development, aging, learning, disease and evolution," *Frontiers in Neuroinformatics*, vol. 3, p. 25, 2009.
- [45] X. Huang and S. Belongie, "Arbitrary style transfer in real-time with adaptive instance normalization," in *CVPR*, 2017, pp. 1501–1510.
- [46] E. Perez, F. Strub, H. De Vries, V. Dumoulin, and A. Courville, "FILM: Visual reasoning with a general conditioning layer," in *AAAI*, 2018.
- [47] T. Park, M.-Y. Liu, T.-C. Wang, and J.-Y. Zhu, "Semantic image synthesis with spatially-adaptive normalization," in *CVPR*, 2019, pp. 2337–2346.
- [48] M. C. H. Lee, K. Petersen, N. Pawlowski, B. Glocker, and M. Schaap, "Tetris: Template transformer networks for image segmentation with shape priors," *TMI*, vol. 38, no. 11, pp. 2596–2606, 2019.
- [49] G. Jacenkow, A. Chatsias, B. Mohr, and S. A. Tsaftaris, "Conditioning convolutional segmentation architectures with non-imaging data," in *MIDL*, 2019.
- [50] A. Chatsias, T. Joyce, G. Papanastasiou, S. Semple, M. Williams, D. E. Newby, R. Dharmakumar, and S. A. Tsaftaris, "Disentangled representation learning in cardiac image analysis," *Medical Image Analysis*, vol. 58, p. 101535, 2019.